Supporting Information

Structural and Bluish-White Luminescent Properties of Li^+-doped BPO_4 as a Potential Environmentally-Friendly Phosphor Material

Cuimiao Zhang, Hongzhou Lian, Deyan Kong, Shanshan Huang, and Jun Lin*

State Key Laboratory of Application of Rare Earth Resources, Changchun Institute of Applied Chemistry, Chinese Academy of Sciences, Changchun 130022, and Graduate University of the Chinese Academy of Sciences, Beijing 100049, P. R. China

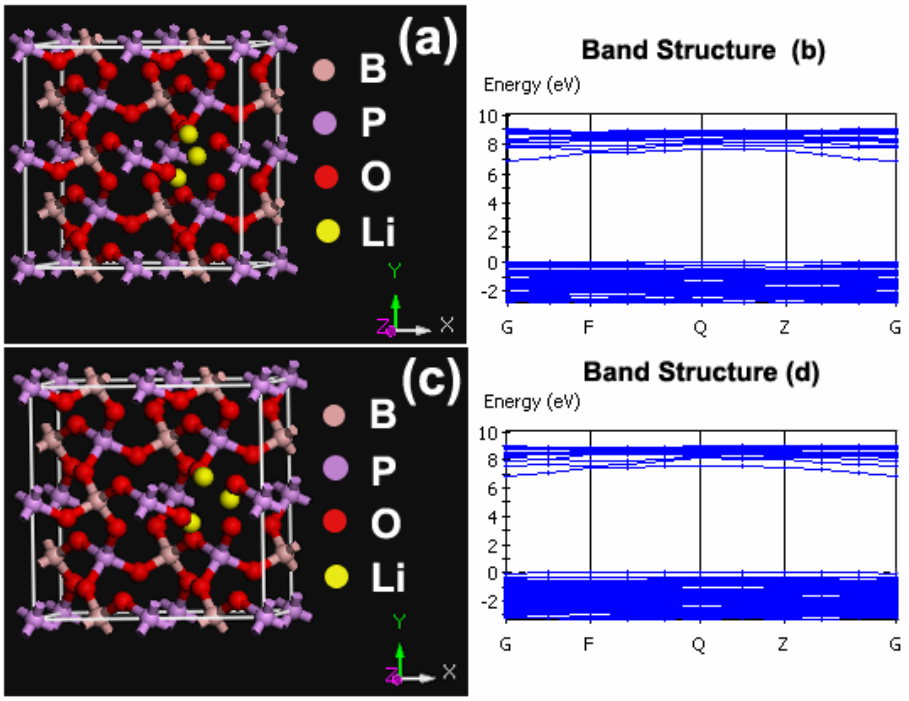

Figure S1. Two possible defect structure models of Li^+-doped BPO_4: Li_B'' + $2Li_i$ (a), V_B''' + $3Li_i$ (c), and the calculated band structures according the models of Li^+-doped BPO_4: Li_B'' + $2Li_i$ (b), V_B''' + $3Li_i$ (d).

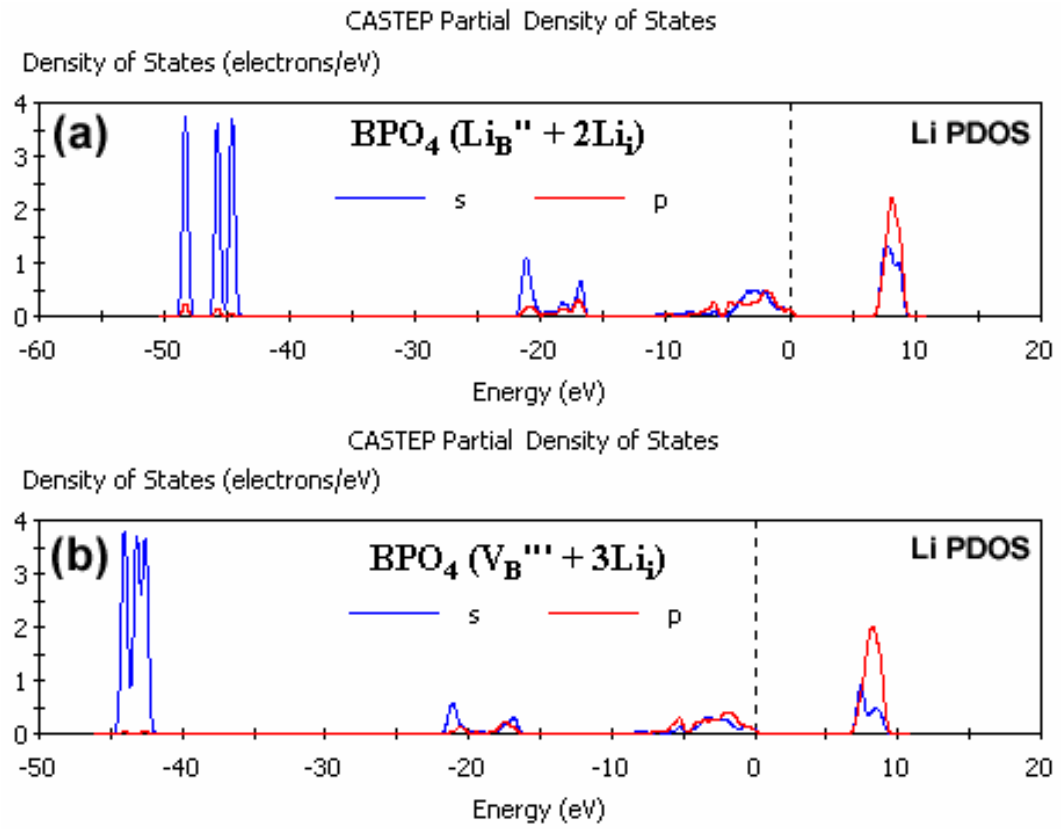

Figure S2. The partial density of states (calculated PDOS) of Li in two possible defect models: (a) BPO_4 with the $Li_B'' + 2Li_i$ defect, (b) BPO_4 with the $V_B''' + 3Li_i$ defect.

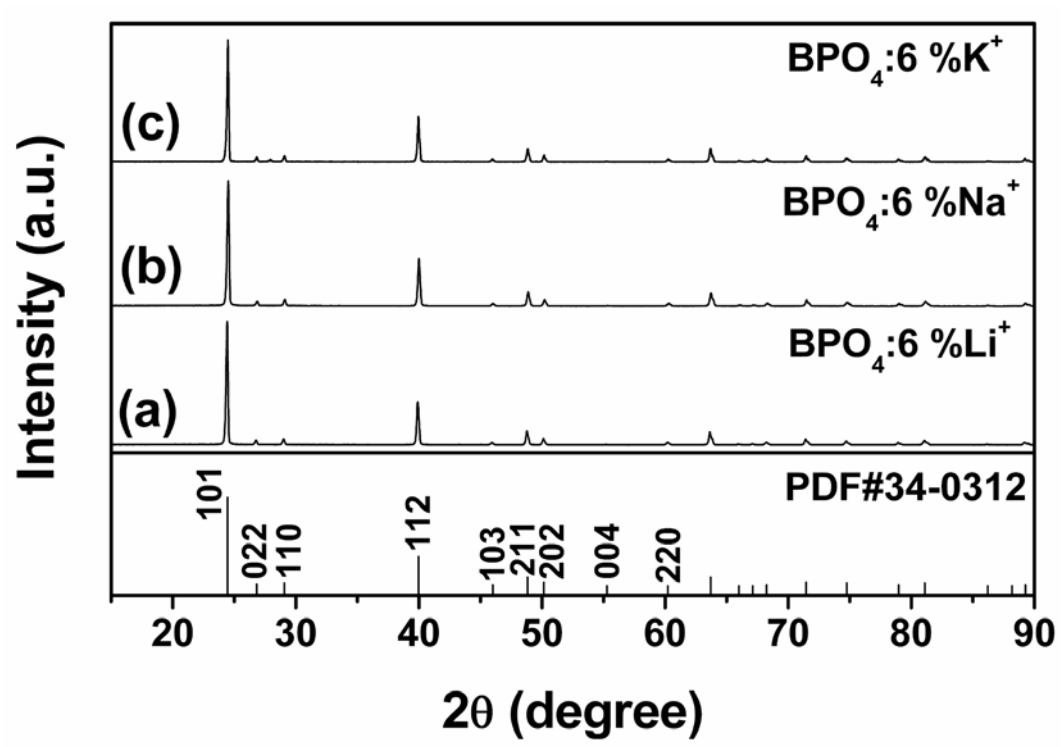

Figure S3. The XRD patterns for PSG-derived BPO_4:6%Li^+ (a), BPO_4:6%Na^+ (b), BPO_4:6%K^+ (c), and the standard data of BPO_4 (JCPDS 34-0132) as a reference. All of the samples were obtained after annealing at 960 ^oC for 3 h.

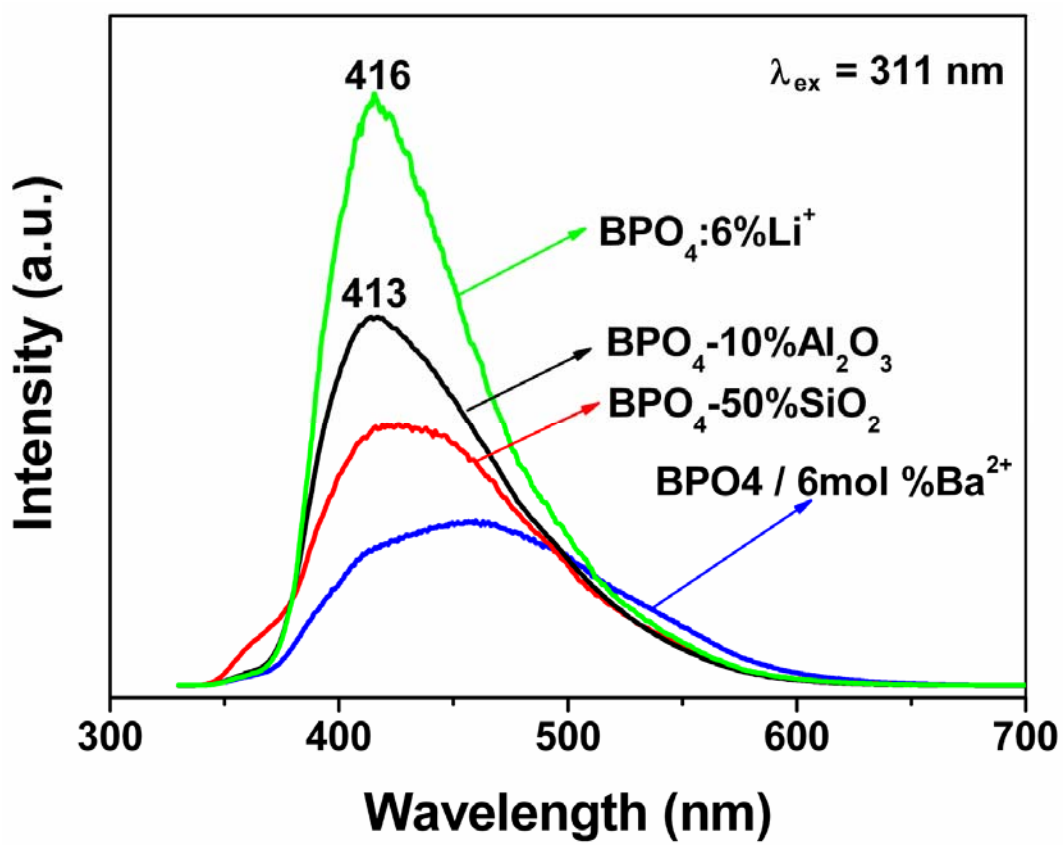

Figure S4. The emission spectra for BPO_4-50%SiO_2 (red line), BPO_4-10%Al_2O_3 (black line), BPO_4 / 6 mol % Ba^{2+} (blue line), and BPO_4:6%Li^+ (green line).

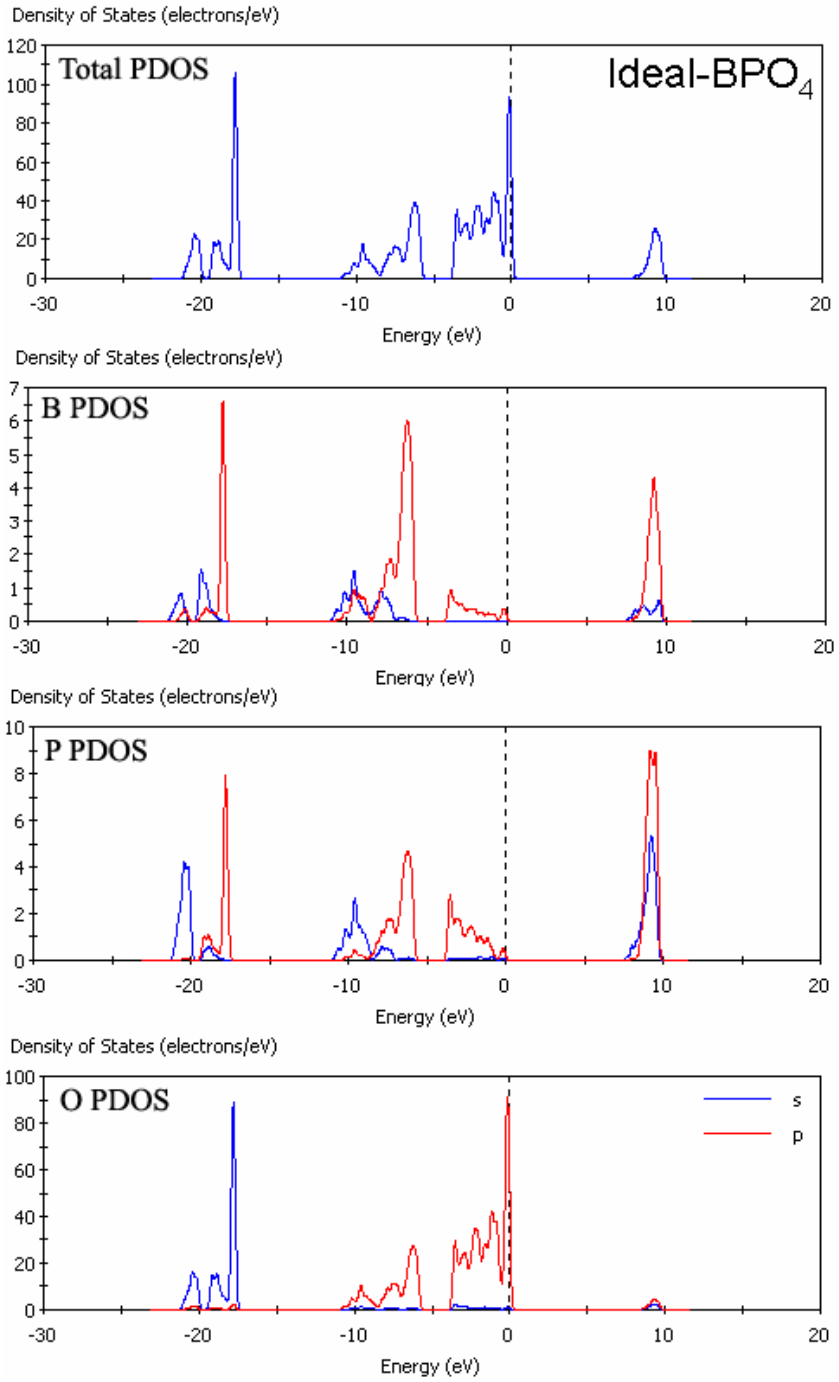

Figure S5. The calculated PDOS of the ideal BPO_4.

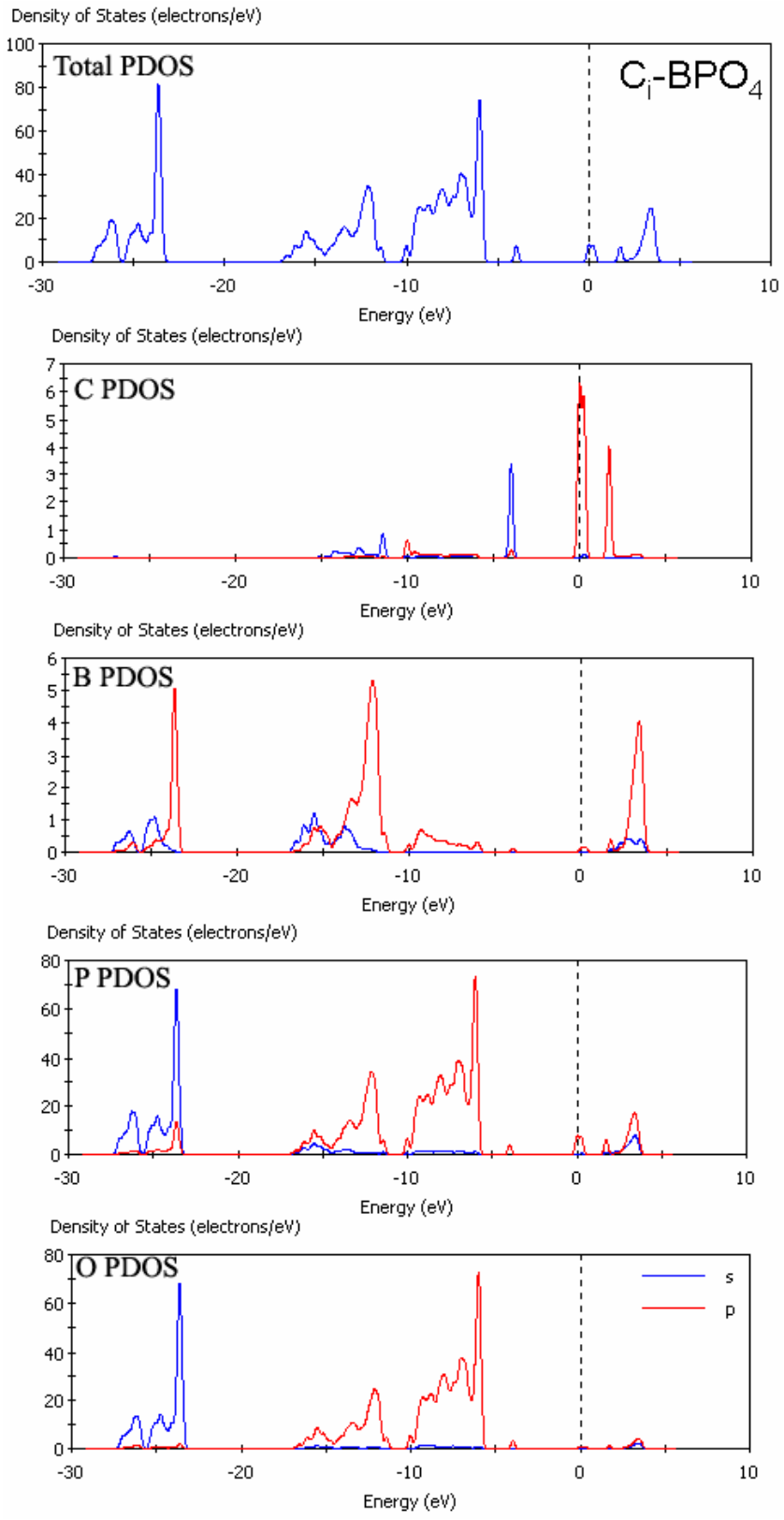

Figure S6. The calculated PDOS of the BPO_4 with the defect of interstitial carbon impurity.

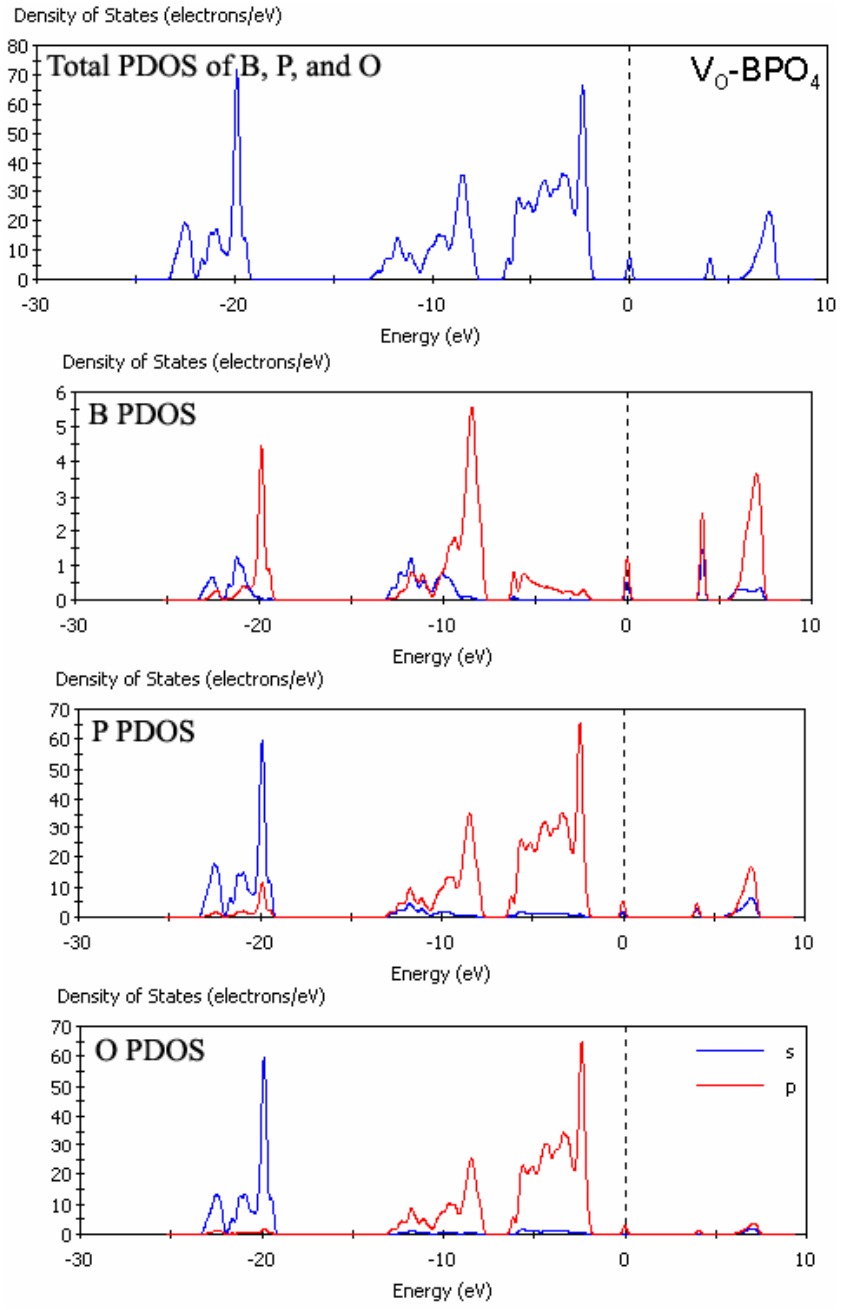

Figure S7. The calculated PDOS of the BPO_4 with the defect of oxygen vacancy.